Highly Accurate Real-Time GPS Carrier Phase-Disciplined Oscillator

Chia-Lung Cheng, Fan-Ren Chang, and Kun-Yuan Tu

***Abstract*—A low-cost highly accurate real-time GPS carrier phase disciplined oscillator system based on a single-frequency receiver is presented. In order to estimate the average frequency offsets of an oven-controlled crystal oscillator (OCXO) with respect to the GPS, the OCXO was connected to a modified GPS receiver to replace its original oscillator. Hence, the behavior of the OCXO was determined from the GPS carrier phase observations. The average frequency offsets of the OCXO with respect to the GPS could be estimated by performing difference operations on carrier phase observations of all satellites in view between two measurement epochs. To overcome the interference coming from the atmospheric delay, a real-time dynamic neural-wavelet forecasting filter was proposed. The parameters of the filter were obtained according to the results of a three-day experiment, in which the GPS carrier phase observations of a stand-alone configuration and a common-view configuration were compared. The compressed average frequency offsets were then used by the neural model predictive controller (MPC) for steering the OCXO via D/A converters. From our experiments, the normalized frequency offset of the disciplined OCXO could be improved from about two parts in 10^9 to about three parts in 10^{14}, and the frequency stability (MDEV) could be improved from about eight parts in 10^{10} to about four parts in 10^{14} over 24 h.**

***Index Terms*—Atmospheric delay, disciplined oscillator, neural-wavelet.**

I. Introduction

THE global positioning system-disciplined oscillator (GPSDO) [1] based on coarse/acquisition (C/A) code observations is one of the principal methods of maintaining highly accurate frequency traceability worldwide. However, GPSDOs are subject to errors and biases caused by signal noise and atmosphere. The capability of using GPS carrier phase rather than C/A code to transfer precise time and frequency has been recognized [2], [3]. Because the frequency of the carrier phase is roughly 1000 times higher than that of C/A code, time and frequency dissemination using the carrier phase have much greater resolution, in principle. To achieve the highest frequency accuracy from the GPS, the atmospheric propagation errors should be compensated for. The ionospheric errors may currently be minimized by a dual-frequency receiver. But this type of receiver is more expensive than a single-frequency receiver. Therefore, we introduce here a low-cost, yet accurate, frequency-disciplined system, composed of a single-frequency receiver with the dynamic neural-wavelet forecasting filter. Single-frequency receivers usually include a correction for the atmospheric delay, based on an ionosphere model and a troposphere model built into the GPS. These models are expected to remove about 40%–75% of the atmospheric effects on average [4]. Since the parameters of these models are estimated in advance and then transmitted to the GPS satellites, they cannot anticipate day-to-day random fluctuations, and thus, cannot be completely accurate in real time. Alternatively, various organizations have developed detailed and accurate models of the atmosphere, based on GPS observations, for single-frequency users to reduce atmospheric effects as much as possible in post-processing [5]. However, some of these models are computationally complex. To compensate for the above drawbacks, we have developed an accurate atmospheric correction with the dynamic neural-wavelet forecasting filter in our real-time disciplined system. The scheme can allow traceability to the international time and frequency standard as disseminated by the GPS. In order to estimate the average frequency offsets of an oven-controlled crystal oscillator (OCXO) with respect to the GPS, the OCXO was connected to a modified GPS receiver to replace its original oscillator. Hence, the behavior of the OCXO was determined from the GPS carrier phase observations. The average frequency offsets of the OCXO with respect to the GPS could be estimated by performing difference operations on carrier phase observations of all satellites in view between two measurement epochs. To overcome the interference coming from the atmospheric delay, a real time dynamic neural-wavelet forecasting filter was proposed. The parameters of the filter were obtained according to the results of a three-day experiment, in which the GPS carrier phase observations of a stand-alone configuration and a common-view configuration were compared. The compressed average frequency offsets were then used by the neural model predictive controller (MPC) for steering the OCXO via D/A converters.

Using the above methods, the OCXO showed that the normalized frequency offset could be improved from two parts in 10^9 to about three parts in 10^{14}, and the frequency stability (MDEV) of the OCXO could be improved from about eight parts in 10^{10} to about four parts in 10^{14} for an averaging time of one day. Our experiments revealed that the proposed architecture is sound and cost effective. The disciplined system has the potential to greatly improve the normalized frequency offset and frequency stability of the low-cost OCXO in real time.

Manuscript received July 2, 2004; revised October 29, 2004.

C.-L. Cheng and F.-R. Chang are with the Department of Electrical Engineering, National Taiwan University, Taipei 10617, Taiwan, R.O.C. (e-mail: charles@ac.ee.ntu.edu.tw).

K.-Y. Tu is with the National Standard Time and Frequency (NSTF) Laboratory, Telecommunication Laboratories, Chunghwa Telecom Company, Ltd., Taipei, Taiwan 326, R.O.C.

Digital Object Identifier 10.1109/TIM.2004.843403

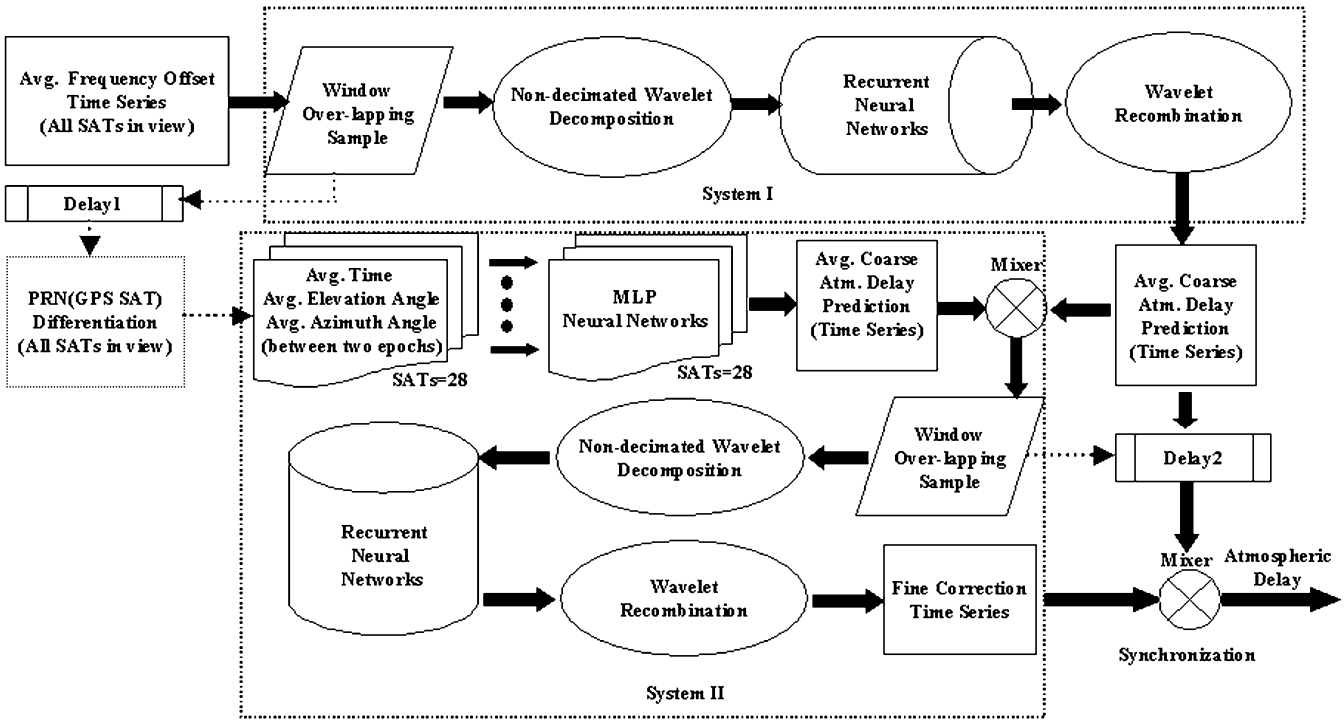

Fig. 1. The functional block diagram of the dynamic neural-wavelet forecasting filter for the correction of atmospheric delay.

II. Dynamic Forecasting Filter of Atmospheric Delay

The dynamic neural-wavelet forecasting filter is split between two main systems. This is illustrated in Fig. 1. System I performs a global approximation of the desired prediction with the real-time limited information which is affected by high noise, nonstationary, and nonlinearity. The series of average frequency offsets between the disciplined oscillator and the GPS represent the input data for System I. The window-overlapping sample is preproceeded with the wavelet technique for use in real time. The window-overlapping sample analyzes only a small section $(2^8 \times \text{sampling interval})$ of the signal and shifts the window with one sampling interval at each new sampling operation. The nondecimated wavelet transforms (NWT) are used as the presignal processor in the neural-wavelet technique. The NWT produces equal-length wavelet coefficients for each resolution level [6]. Depending on the selected resolution level, the signals are decomposed into a number of wavelet coefficients. The functions of the NWT are equivalent to those of a series of lowpass filters. The result obtained at the output of each filter is the approximation (low-frequency information) coefficient series and detail (high-frequency information) coefficient series. The resolution level of the proposed filter is eight. The outputs of the NWT include one approximation coefficient series and eight detail coefficient series. Recurrent neural networks (RNNs) of System I are used for coarse atmospheric prediction. The number of RNNs needed here is nine. Finally, the outputs from RNNs are recombined, using the NWT technique and the same resolution level, to form the predicted atmospheric delay for System I. The use of recurrent neural networks is also important for our system because RNNs can take into account the greater history of the input [7]. The RNN is a two-layer network with one input node, seven hidden nodes, seven recurrent nodes, and one output node. The network has a tangent sigmoid transfer function in its hidden and recurrent layers. The network has a linear transfer function in its output layer. The desired output of system I is the atmospheric delay interfered frequency offset sequence when the oscillator's initial frequency offset is zero.

The purpose of System II is to fine-tune the results of System I. A local approximation approach is performed here. Two sets of neural networks are included. The configuration of the first set is the multilayer perception neural network (MLPNN). The number of MLPNNs is equal to the number of visible GPS satellites. For each MLPNN, there are three input nodes, eight hidden nodes, and one output node. The inputs of every MLPNN include three types: average time, average elevation angle, and average azimuth angle between two measurement epochs for the associated GPS satellites. The output of the MLPNN is the trend of average atmospheric delay. The configuration of the second set neural network in System II is similar to that of System I. It is a neural-wavelet-based structure. Its input is the difference between the output of System I and the average forecasted atmospheric delay of the MLPNNs. Due to the operations of this neural-wavelet filter, a fine calibration of the atmospheric effects is computed. The output of System II is the desired frequency offset sequence of the oscillator, not interfered with by atmospheric delay.

Finally, a better atmospheric delay sequence can be made available by the difference operations between the output of System I and the output of System II.

The results of a three-day experiment, in which GPS carrier phase observations of a stand-alone configuration and a common-view configuration were stored, were used to determined the parameters of all the neural networks of the forecasting filter. According to the desired output of each neural

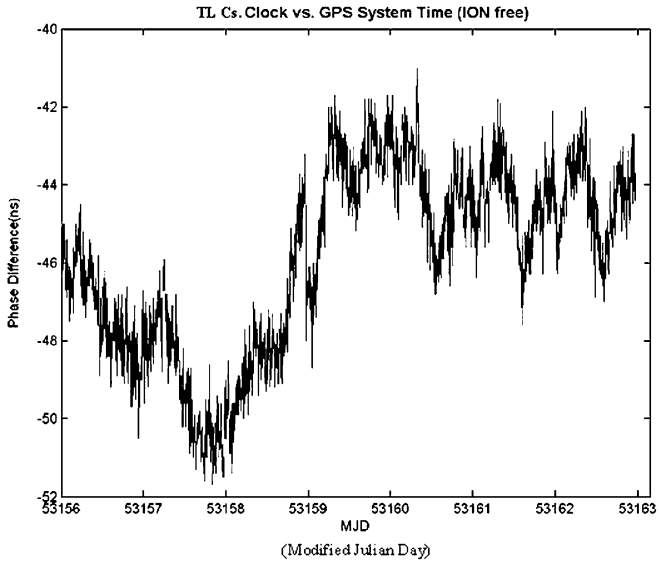

Fig. 2. The phase difference estimation between the TL cesium clock and the GPS using the dual-frequency method for ION-delay free.

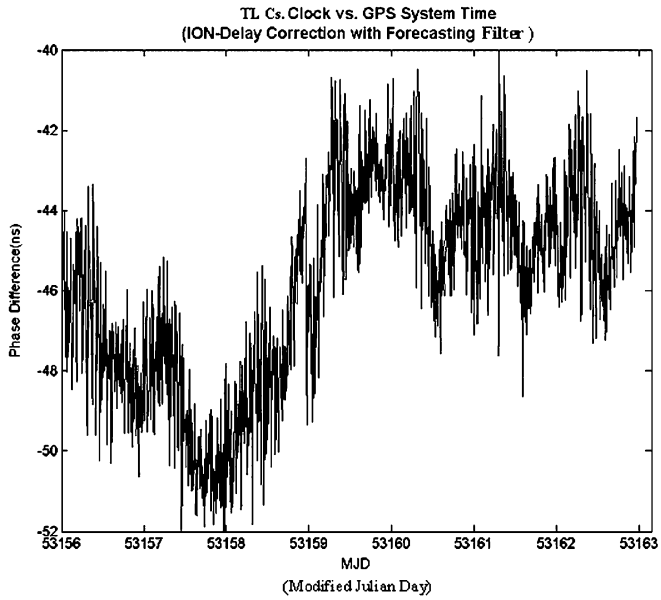

Fig. 3. The phase difference estimation between the TL cesium clock and the GPS using the dynamic forecasting filter for the real-time correction of ION-delay.

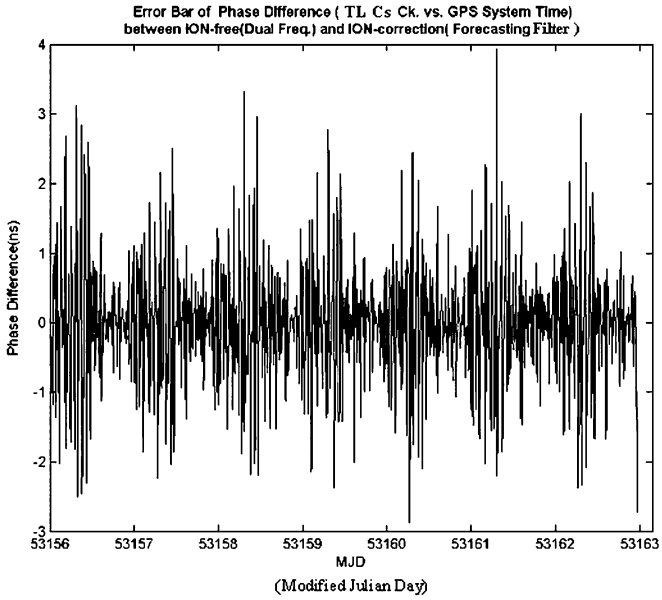

Fig. 4. The error bar estimation of the phase difference between the dual-frequency method and the dynamic forecasting filter.

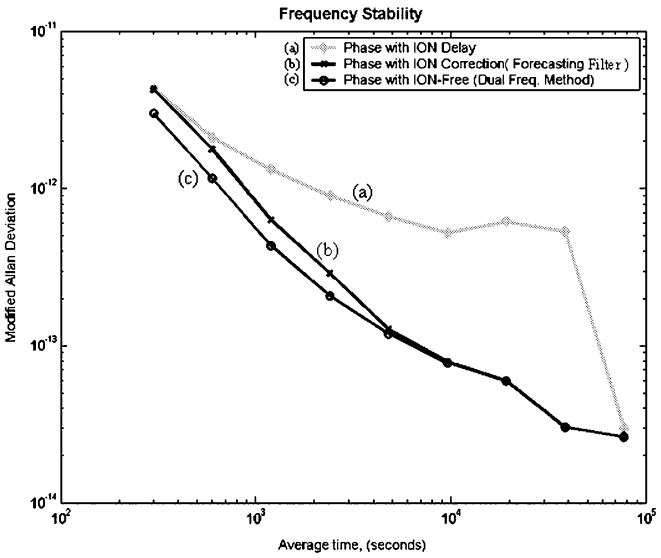

Fig. 5. The frequency stability comparison using both ways (the dual-frequency method and the dynamic forecasting filter) of the ION-delay correction and without ION-delay correction.

network, the typical adaptive methods were applied to set the weights and biases of each layer.

To verify the ability of our dynamic forecasting filter, the data using the GPS-smoothed P3 code is preliminarily processed. Now, the ionosphere (ION)-free effect of the dual-frequency method is the training goal for our forecasting filter. We use the information of the past three days to tune our forecasting filter. Then, we simultaneously adopt the dual-frequency method and our filter to correct the phase difference data between the Telecommunication Laboratories (TL) cesium (Cs) clock and the GPS for seven days. The phase difference estimations using these two methods are shown separately in Figs. 2 and 3. Fig. 4 represents the differences between Figs. 2 and 3. Fig. 5 expresses the frequency stability analysis. The comparisons of the above two methods are listed in Table I. The phase difference estimates between the TL Cs clock and the GPS are similar in the dual-frequency method and our forecasting filter method. From the traditional statistics (maximum, minimum, average, medium, standard deviation) and Allan deviation ($\tau = 300$ s), we can find that the measured noises of the TL Cs clock using both methods are similar. In addition, we use the approach for power law noise identification [8] based on the lag 1 autocorrelation function to determine the dominant noise types of the two sets of data, the set from the dual-frequency method and that from our forecasting method. The results show that their dominant noise types are the same one: flicker phase modulation (FPM). Finally, the estimations of normalized frequency offsets are almost the same. The results indicate that

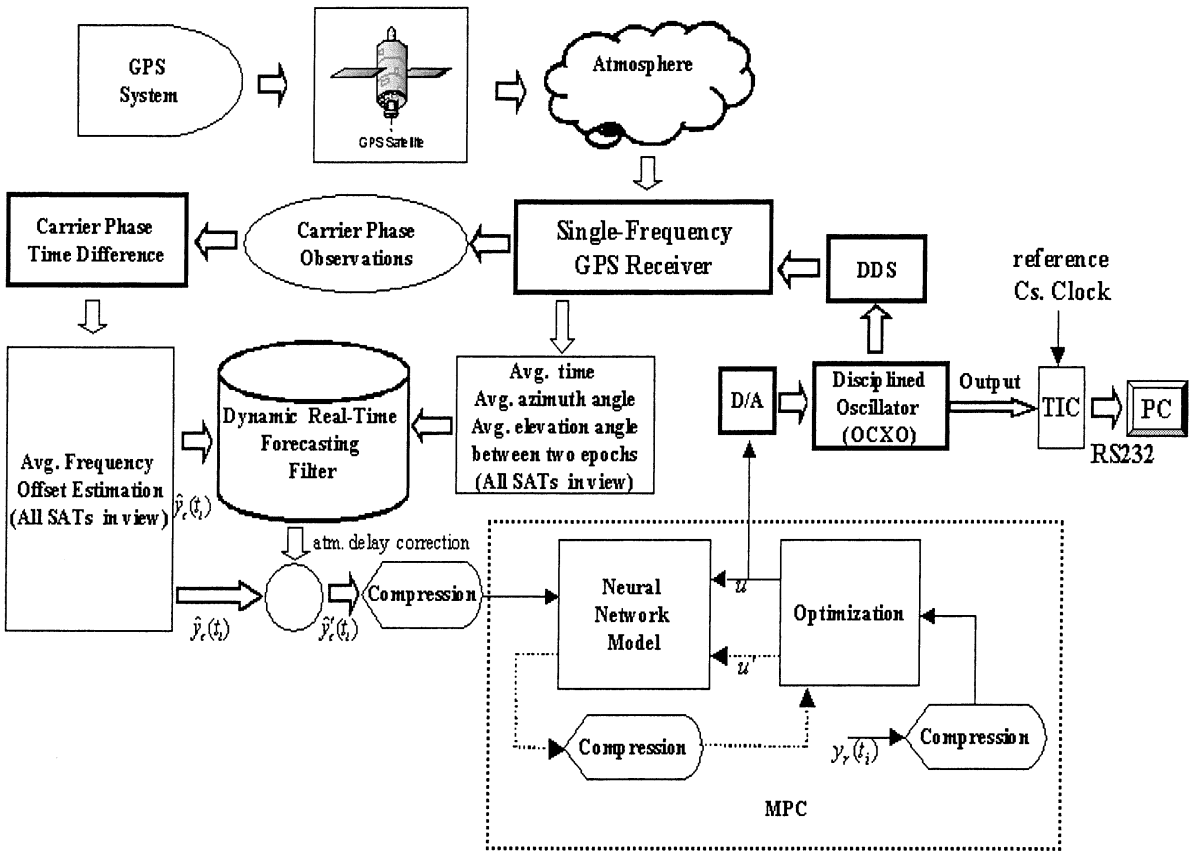

Fig. 6. The real-time system architecture for the GPS carrier phase disciplined oscillator.

TABLE I
THE COMPARISONS OF STATISTICS BETWEEN THE ION-DELAY CORRECTION OF THE DYNAMIC NEURAL-WAVELET FORECASTING FILTER AND THE ION-DELAY FREE USING A DUAL-FREQUENCY METHOD

Phase Data	Dual Frequency Method	Dynamic Forecasting Filter
Max.	-4.12×10^{-8} sec.	-3.95×10^{-8} sec.
Min.	-5.17×10^{-8} sec.	-5.22×10^{-8} sec.
Avg.	-4.58×10^{-8} sec.	-4.58×10^{-8} sec.
Median	-4.54×10^{-8} sec.	-4.52×10^{-8} sec.
Std. Deviation	2.51×10^{-12}	3.81×10^{-12}
Sigma(Allan,5min.)	3.01×10^{-12}	4.29×10^{-12}
Noise	FPM	FPM
Lag 1 autocorrelation	Alpha= +1.14	Alpha= +0.84
Frequency Offset (Linear Fit)	2.63×10^{-12}	2.61×10^{-12}

our dynamic forecasting filter has the ability to perform for seven days. Next, we introduced the forecasting filter into the proposed disciplined oscillator system to correct the real-time atmospheric effects on carrier phase.

III. EXPERIMENTAL RESULTS

The functional block diagram of our disciplined system is shown in Fig. 6. The low-cost single-frequency GPS receiver installed in our system was not designed for time and frequency applications. It had no interface ports for external oscillators. In order to use the receivers to establish the system, we replaced the internal quartz oscillator of the receiver with the disciplined oscillator, i.e., OCXO, and connected the receiver through a direct digital synthesizer (DDS). The specifications of the OCXO are as follows: normalized frequency offset, about 1 part in 10^9; frequency stability, about 1 part in 10^{10} over 24 hours; and frequency drift, about 5 parts in 10^{11} per day. The software, including the model predictive controller, the dynamic forecasting filter, and the communication interface between the time interval counter (TIC) and a PC, which was used for data collection, were programmed in C++ and executed on a mobile computer. To find the normalized frequency offset and frequency stability via modified Allan deviation (MDEV), phase comparison is performed between the one pulse per second signals supplied by the OCXO and the reference Cs clock. The specifications of the reference Cs clock are as follows: normalized frequency offset, about four parts in 10^{12}; frequency stability, about eight parts in 10^{14} over 24 hours; and frequency drift, about one part in 10^{16} per day. The coordinates of the GPS antenna were predetermined by the International GPS Service. In order to estimate the frequency offset of the OCXO with respect to the GPS, the OCXO was connected to the modified GPS receiver. With the help of the DDS, the signal of the OCXO could be appropriately converted and supplied to the GPS receiver. Hence, the performance of the OCXO was determined from the GPS carrier phase observations. With the help of the dynamic real-time forecasting filter, the atmospheric delay effects were removed from the average frequency offsets of the OCXO. The compressed average frequency offsets were then used by the neural model predictive controller (MPC) [9] for steering the OCXO via D/A converters. An incremental

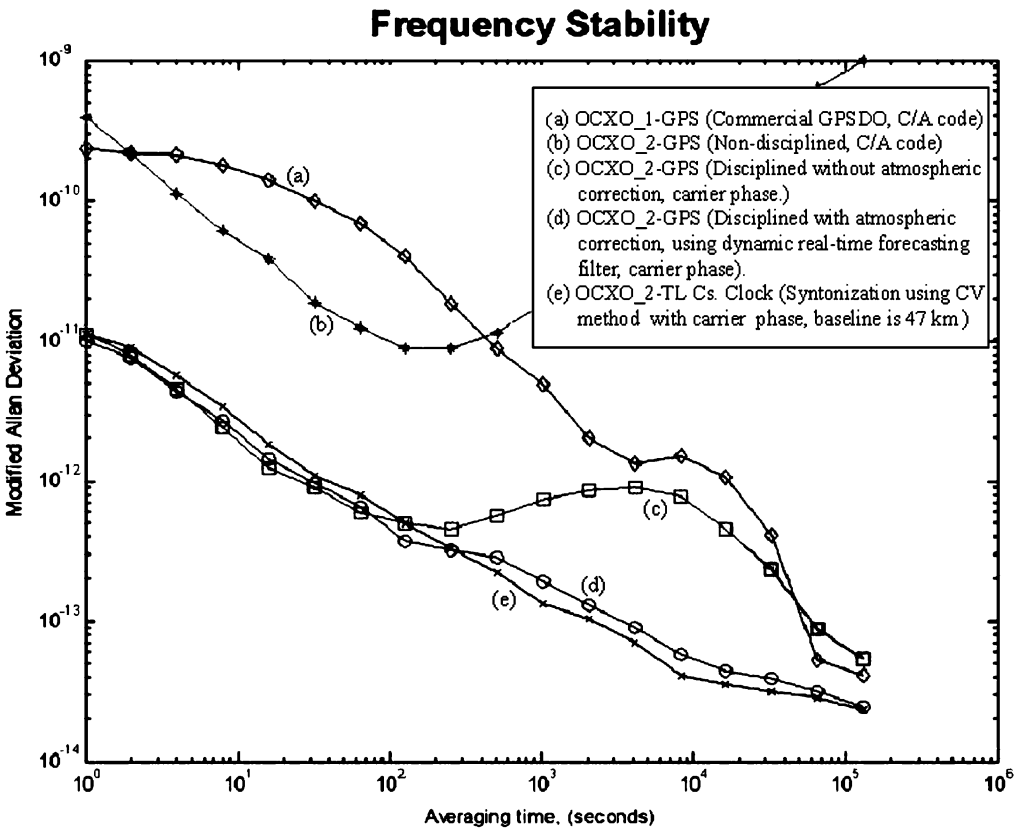

Fig. 7. The frequency stability comparison of the commercial GPSDO, the nondisciplined OCXO, the disciplined OCXO without atmospheric delay correction, the disciplined OCXO with the atmospheric correction of the forecasting filter, and the syntonization using the common view (CV) method between the OCXO and TL cesium clock.

voltage was updated to discipline the OCXO. The control signals (time constant = 1 s) minimize the following performance criterion over the specified horizon.

$$J = \sum_{k=N_1}^{N_2} (y_m(t+k) - y_r(t+k))^2 + \rho \sum_{k=1}^{N_u} (u'(t+k-1) - u'(t+k-2))^2 \quad (1)$$

where N_1, N_2, and N_u define the horizons over which the tracking error and the control increments are evaluated. The u' variable is the tentative control signal, y_r is the desired response, and y_m is the network model response. The value ρ determines the contribution of the sum of the squares of the control increments to the performance index.

Finally, we examined the performance of the commercial GPSDO, the nondisciplined OCXO, the disciplined OCXO without atmospheric delay correction, the disciplined OCXO with the atmospheric correction of the forecasting filter, and the syntonization using the common-view (CV) method between the OCXO and TL Cs clock. The frequency stability analysis is shown in Fig. 7. The frequency stability of the OCXO without the atmospheric delay correction is significantly degraded over the medium term as well as in the long term. Fig. 8 shows the phase difference (zero mean) between the nondisciplined OCXO and the reference Cs clock. The normalized frequency offset of the OCXO is about 2.4×10^{-9} for an averaging time of about one day. Fig. 9 presents the phase difference (zero mean) between the reference Cs clock and the disciplined OCXO with atmospheric effects. The normalized frequency offset of the OCXO is about 5.4×10^{-13} for an averaging time of about one day. Fig. 10 presents the phase difference (zero mean) between the reference Cs clock and the disciplined OCXO

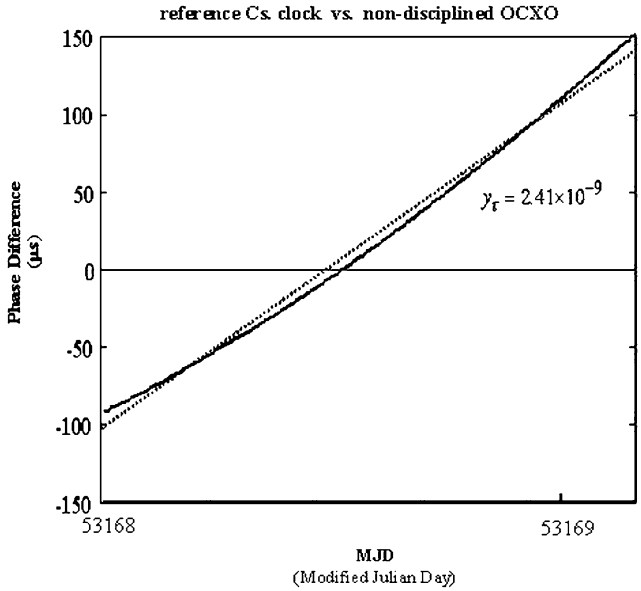

Fig. 8. The phase difference between the reference cesium clock and nondisciplined OCXO with linear-fit line.

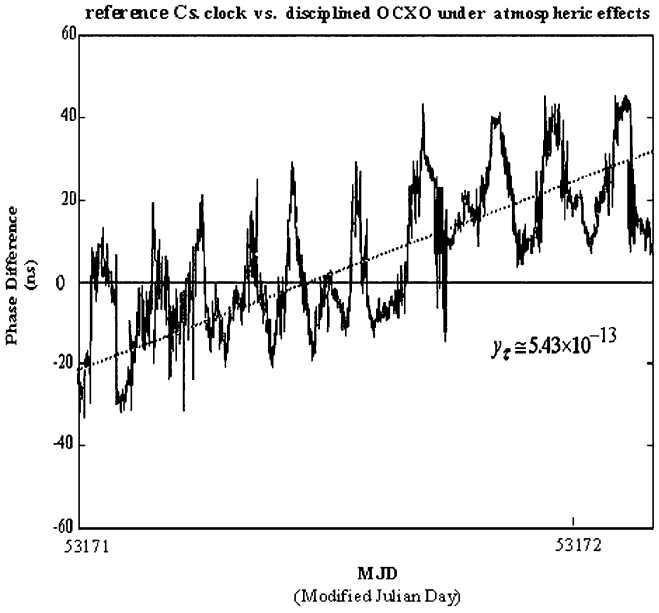

Fig. 9. The phase difference between the reference cesium clock and the disciplined OCXO (MPC) under atmospheric effects with linear-fit line.

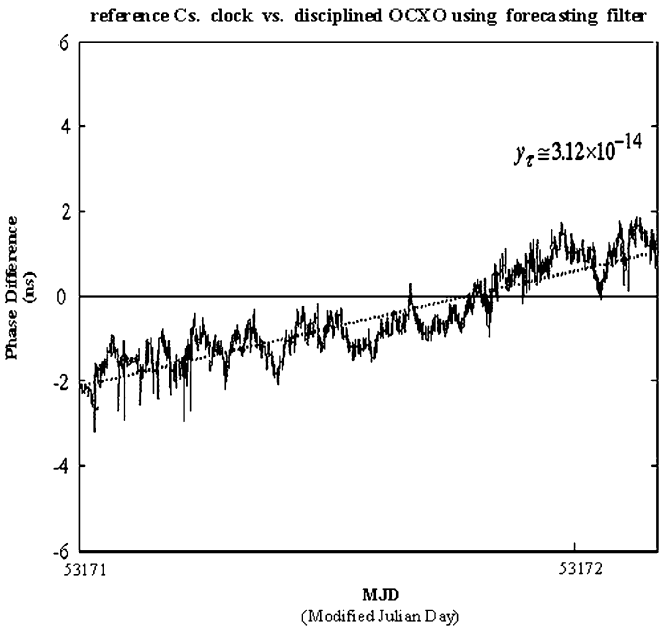

Fig. 10. The phase difference between the reference cesium clock and the disciplined OCXO (MPC) using the atmospheric delay correction of the forecasting filter with linear-fit line.

with atmospheric delay correction by the proposed forecasting filter. The normalized frequency offset of the OCXO is about 3.1×10^{-14} for an averaging time of about one day.

IV. Conclusion

In this paper, a new low-cost, highly accurate real-time GPS carrier phase-disciplined system based on a single-frequency receiver and the atmospheric forecasting filter is presented. The scheme can allow traceability to the international time and frequency standard as disseminated by the GPS. In addition, we observed that the model predictive control of the neural network is robust and adaptive for our disciplined system. Three improvements and advantages in our methodology are provided. First, we have developed a forecasting filter to correct for atmospheric delay in real time. The filter is available easily and anticipative day-to-day. Second, the low-cost OCXO can be disciplined to obtain highly normalized frequency offset and frequency stability in the short term as well as in the long term. Experimental results show that the stability (MDEV) over 1 s was 9.2×10^{-12}. Compared with the commercially available GPS disciplined oscillator (GPSDO), the short-term stability (MDEV, $\tau = 1$ s) of our design was about ten times better. Moreover, the stability improvement of the disciplined OCXO in the medium and long term was caused by our atmospheric correction. Third, the frequency performance of the disciplined system, with the use of a low-cost GPS receiver, an inexpensive OCXO, and the dynamic neural-wavelet forecasting filter of atmospheric delay, was almost as good as that of a commercial atomic clock. Therefore, the disciplined system is sound, reliable and cost effective.

References

[1] J. Davis and J. M. Furlong, "A study examining the possibility of obtaining traceability to UK national standards using GPS disciplined oscillators," in *Proc. 11th European Frequency Time Forum*, 1997, pp. 515–520.

[2] R. Dach *et al.*, "Continuous time transfer using PGPS carrier phase," *IEEE Trans. Ultrason., Ferroelectr., Freq. Control*, vol. 49, no. 11, pp. 1480–1490, Nov. 2002.

[3] J. Ray and K. Senior, "IGS/BIPM pilot project: GPS carrier phase for time/frequency transfer and time scale formation," *Metrologia*, vol. 40, pp. 270–288, 2003.

[4] B. Hofmann-Wellenhof, H. Lichtenegger, and J. Collins, *Global positioning system: Theory and practice*, 4th ed. New York: Springer-Verlag, 1997, pp. 99–109.

[5] J. Ray, "New timing products from the IGS: IGS/BIPM time transfer pilot project and UT1-like estimates from GPS," in *Proc. IVS Meeting*, 2000, p. 289.

[6] G. Zhang *et al.*, "Wavelet transform for filtering financial data streams," *J. Computational Intelligence Finance*, vol. 7, no. 3, pp. 18–35, May/Jun. 1999.

[7] C. Lee Giles, S. Lawrence, and A. C. Tsoi, "Noisy time series prediction using a recurrent neural network and grammatical inference," *Mach. Learn.*, vol. 44, pp. 161–183, Jul./Aug. 2001.

[8] W. J. Riley and C. A. Greenhall. Power law noise identification using the lag 1 autocorrelation. presented at Proc. 18th Eur. Frequency Time Forum (EFTF). [Online] Available: http://www.wriley.com/Paper125Preprint.pdf

[9] D. Soloway and P. J. Haley, "Neural generalized predictive control," in *Proc. IEEE Int. Symp. Intelligent Control*, 1996, pp. 277–281.